

Urethral identification using three-dimensional magnetic resonance imaging and interfraction urethral motion evaluation for prostate stereotactic body radiotherapy

Yutaka Kato¹, Shintaro Okumiya¹, Kuniyasu Okudaira¹, Junji Ito²,
Motoki Kumagai², Takeshi Kamomae², Yumiko Noguchi¹,
Mariko Kawamura², Shunichi Ishihara² and Shinji Naganawa²

¹Department of Radiological Technology, Nagoya University Hospital, Nagoya, Japan
²Department of Radiology, Nagoya University Graduate School of Medicine, Nagoya, Japan

ABSTRACT

Prostatic urethra identification is crucial in prostate stereotactic body radiotherapy (SBRT) to reduce the risk of urinary toxicity. Although computed tomography (CT) with a catheter is commonly employed, it is invasive, and catheter placement may displace the urethral position, resulting in possible planning inaccuracies. However, magnetic resonance imaging (MRI) can overcome these weaknesses. Accurate urethral identification and minimal daily variation could ensure a highly accurate SBRT. In this study, we investigated the usefulness of a three-dimensional (3D) T2-weighted (T2W) sequence for urethral identification, and the interfractional motion of the prostatic urethra on CT with a catheter and MRI without a catheter for implementing noninvasive SBRT. Thirty-two patients were divided into three groups. The first group underwent MRI without a catheter to evaluate urethral identification by two-dimensional (2D)- and 3D-T2W sequences using mean slice-wise Hausdorff distance (MSHD) and Dice similarity coefficient (DSC) of the contouring by two operators and using visual assessment. The second group provided 3-day MRI data without a catheter using 3D-T2W, and the third provided 3-day CT data with a catheter to evaluate the interfractional motion using MSHD, DSC, and displacement distance (Dd). The MSHD and DSC for the interoperator variability in urethral identification and visual assessment were superior in 3D-T2W than in 2D-T2W. Regarding interfractional motion, the Dd value for prostatic urethra was smaller in MRI than in CT. These findings indicate that the 3D-T2W yielded adequate prostatic urethral identification, and catheter-free MRI resulted in less interfractional motion, suggesting that 3D-T2W MRI without a catheter is a feasible noninvasive approach to performing prostate SBRT.

Keywords: prostatic urethra, catheter, magnetic resonance imaging, computed tomography, interfractional motion

Abbreviations:

CT: computed tomography
DSC: dice similarity coefficient
MRI: magnetic resonance imaging
MSHD: mean slice-wise Hausdorff distance
ROI: region of interest

Received: June 9, 2022; accepted: September 15, 2022

Corresponding Author: Shintaro Okumiya, MS

Department of Radiological Technology, Nagoya University Hospital,
65 Tsurumai-cho, Showa-ku, Nagoya 466-8560, Japan

Tel: +81-52-744-2566, Fax: +81-52-744-2559, E-mail: okumiyas@med.nagoya-u.ac.jp

SBRT: stereotactic body radiotherapy
T2W: T2-weighted
2D: two-dimensional
3D: three-dimensional

This is an Open Access article distributed under the Creative Commons Attribution-NonCommercial-NoDerivatives 4.0 International License. To view the details of this license, please visit (<http://creativecommons.org/licenses/by-nc-nd/4.0/>).

INTRODUCTION

Prostatic urethra identification is crucial in stereotactic body radiotherapy (SBRT) for prostate cancer because urethral dose reduction can reduce the risk of urinary toxicity, such as frequency, dysuria, and urethral stricture, without significantly increasing the risk of local recurrence.^{1,2} Because urethral visualization is difficult by computed tomography (CT), there are two strategies for achieving this goal: one is urinary catheter insertion, which is commonly employed^{1,3-5} and recommended by GEC/ESTRO.⁶ However, catheterization every time for multiple days of irradiation is invasive and associated with a risk of infection, and is undesirable for patients. The incidence of bacteriuria associated with indwelling catheterization is 3%–8% per day.⁷ Although the risk of infection may be small,⁸ a previous study revealed that the Foley catheter-related genitourinary trauma was as common as symptomatic urinary tract infection and concluded that the elimination of unnecessary Foley catheterization could prevent symptomatic urinary tract infection, unnecessary antimicrobial therapy for asymptomatic bacteriuria, and Foley catheter-related trauma.⁹ Another is that catheter insertion during radiotherapy must be performed by oncologists or radiology nurses who are unfamiliar with the procedure, which may increase patient discomfort and infection risk. Furthermore, urethral catheter placement may displace the urethral position,^{10,11} and removal of a catheter may cause prostate rotation,¹² resulting in possible planning inaccuracies. As another strategy without using a catheter, a previous study advocated the concept of placing a “surrogate urethra” in the anatomic center of the prostate if the location of the urethra cannot be visualized.¹³ However, another study demonstrated that the urethral dose might be overestimated when using a surrogate urethra,¹⁴ and there were cases where the urethra was not located in the anatomical center of the prostate.^{14,15} Therefore, clear urethral visualization using a clinical image is desirable for accurate radiation treatment planning.

Magnetic resonance imaging (MRI) is increasingly used in radiation treatment planning because of its superior soft tissue contrast^{16,17} and may be suitable for urethral identification purposes.¹⁶ Several studies have investigated urethral identification using MRI; however, they used only two-dimensional (2D) T2-weighted (T2W) turbo spin-echo (TSE) imaging.^{15,18-20} A previous study proposed MRI while urinating; however, there were some problems regarding the psychological burden on patients and the urine bag used to collect urine.¹⁹ To overcome these drawbacks, Yoshimura et al demonstrated that it was possible to identify the prostatic urethra using “posturination” MRI with good accuracy.²⁰ However, there are disadvantages like the bladder volume does not match that of CT imaging and the accuracy is inferior to that of CT with catheter insertion. These limitations indicate that there is not yet a complete approach for prostatic urethral identification noninvasively.

According to the prostate imaging reporting and data system (PI-RADS) guidelines,²¹ 2D T2W-TSE is a key sequence for diagnostic prostate MRI. However, recent advances have shown that three-dimensional (3D) T2W-TSE sequences are more readily achievable with a clinically acceptable acquisition time.²² Some studies have directly compared 2D- and 3D-T2W sequences, focusing on image quality and tumor detection mainly for diagnostic purposes in prostate MRI, and have shown the usefulness of 3D sequences.^{23,24} Additionally, some studies have

utilized 3D-T2W images for prostate contouring in radiation treatment planning.^{16,17} Therefore, we hypothesized that a 3D-T2W image would allow for more accurate urethral identification compared with 2D-T2W.

Another interest in prostate SBRT is the interfractional motion (ie, daily variation) of prostatic urethra position, which is a key factor in the success of urethral-sparing radiotherapy. If the prostatic urethral original position varies from day-to-day, the dose delivered to the urethra will deviate from the planning. To avoid over irradiation due to displacement of the prostatic urethra, replanning must be performed, which is time-consuming and labor intensive. It is ideal to perform daily irradiation with the same planning at all times, with minimal (or no) variation in the daily urethral position. However, a previous study suggested the possibility of catheter-induced displacement of the prostatic urethra.¹⁰ Further, we have treated clinical cases at our institution that required replanning due to displacement of the urethra by catheter insertion. Therefore, we expected that the absence of catheter insertion would lead to less interfractional motion than catheter CT; however, to our knowledge, no report has investigated the interfractional motion of the prostatic urethra.

The purpose of this study was twofold: to demonstrate the usefulness of 3D-T2W images for more accurate prostatic urethral identification and to investigate the interfractional motion of prostatic urethra on CT with a catheter and MRI without a catheter, toward the implementation of noninvasive prostate SBRT without catheter insertion.

MATERIALS AND METHODS

Patient data

The observational study was approved by the ethics committee of Nagoya University Hospital in Aichi, Japan. Informed consent was waived by the committee because clinical MRI data were collected retrospectively. The total number of included subjects was 32 male patients with prostate cancer who received radiotherapy from May 2020 to May 2021 at our institution. They were categorized into three groups. The first group included 12 patients (mean age, 69.5 years; range, 57–81 years) who had an MRI scan without a catheter for brachytherapy. These data were used to compare the urethral identification in 2D- and 3D-T2W images. The second group included 10 patients (mean age, 70.5 years; range, 59–84 years) who underwent an MRI scan without a catheter for intensity-modulated radiation therapy. These data were used to evaluate the interfractional motion in MRI without a catheter. The third group included 10 patients (mean age, 68.5 years; range, 59–80 years) who underwent a CT scan with a catheter for SBRT. These data were used to evaluate the interfractional motion in CT with a catheter. It was also used as comparative reference data for evaluating urethral identification using MRI.

Image acquisition

All MRI scans were performed on a 3T scanner (MAGNETOM Skyra, Siemens, Erlangen, Germany) using an 18-channel body and spine matrix coil. In the first group, MRI scan without catheter insertion was performed using 2D- and 3D-T2W sequences for dose calculation of brachytherapy. The 2D-T2W sequence was set as the recommended acquisition parameters by the PI-RADS document. Contrarily, regarding 3D-T2W, sampling perfection with application-optimized contrasts using different flip-angle evolutions (SPACE) sequence²⁵ was employed, and used vendor-recommended ordinary acquisition parameters similar to those set in several previous studies^{23,24} investigating 3D-T2W sequence. The detailed acquisition parameters are summarized in Table 1.

Table 1 Detailed acquisition parameters

	2D T2W–TSE	3D T2W–SPACE
Repetition time (ms)	6000	1500
Echo time (ms)	96	140
Flip angle (°)	150	140 (constant)
Field-of-view (mm)	200 × 200	300 × 300
Matrix (phase × read)	292 × 512	307 × 384
Resolution (mm)	0.69 × 0.39	0.98 × 0.78
Slice thickness (mm)	3	0.8
Bandwidth (Hz/Pixel)	264	651
Number of slices	36	224
Number of averages	1	1
Parallel imaging	GRAPPA of 2	GRAPPA of 4
Orientation	Axial	Coronal
Acquisition time (m:sec)	3:30	6:35

2D: two-dimensional

3D: three-dimensional

T2W–TSE: T2-weighted turbo spin-echo

SPACE: sampling perfection with application-optimized contrasts using different flip-angle evolutions

GPAPPA: generalized autocalibrating partially parallel acquisitions

In the second group, an MRI scan without a catheter was performed for 3 days using a 3D-T2W sequence to check the reproducibility of the pelvic anatomical position in planning for intensity-modulated radiation therapy. On each day, MRI acquisition was performed with the same waiting time after urination and with the bladder volume as similar as possible.

All scans for the third group were performed on a CT scanner (SOMATOM Confidence RT Pro, Siemens, Erlangen, Germany) with a resolution of 512 × 512 matrix with a slice thickness of 1.0 mm. All patients in the third group underwent 5 days of SBRT. CT imaging with a catheter was obtained before each day's irradiation to check the urethral position, the fiducial markers, and the condition of stool and bowel gas. A radiation oncologist placed the catheter through the urethra into the bladder for accurate urethral identification, and bladder volume was controlled by infusing saline into the bladder before the CT scan. Note that CT used data from the first 3 days to compare the same number of days as the MRI for the second group. All CT and MR images were acquired according to routine clinical examinations of our institution, and the data were analyzed retrospectively.

Image analysis

A radiation oncologist and medical physicist with extensive experience in radiotherapy, who was blinded to the clinical data and acquisition techniques, performed contouring for prostatic urethral independently. The radiation oncologist contoured the prostatic urethra in all CT and MR images and defined the boundaries of the intraprostatic urethra. The medical physicist performed contouring on the CT images (only on the first day of the third group), and 2D- and 3D-MRI (first group) to evaluate the interoperator variability in urethral identification. According to our

standard routine method in clinical practice, the prostatic urethra was contoured in a 4.0-mm diameter region of interest (ROI) for MRI without a catheter and in a 5.0-mm diameter ROI for CT. Additionally, both operators individually scored the prostatic urethral identification in 2D- and 3D-T2W images as a subjective evaluation on a four-point scale (1 = non-identifiable; 2 = obscured, some effect on contouring; 3 = acceptable, no effect on contouring; 4 = clearly identifiable). In cases of interobserver disagreement, final decisions were reached by consensus.

We performed all contouring and subsequent analysis using MIM Maestro (MIM software ver. 6.9.4, EURO MEDITECH CO, LTD). Mean slice-wise Hausdorff distance (MSHD) and Dice similarity coefficient (DSC) were calculated to compare the interoperator variability for urethral identification as an objective evaluation in CT images, 2D- and 3D-T2W images. MSHD is defined as the maximum nearest neighbor Euclidean distance between the surfaces of the two contours in one slice. DSC of 1 equals perfect agreement overlap, and DSC of 0 equals no agreement. For analyses of interfractional motion, furthermore, automatic rigid registration with the entire prostate as the ROI was conducted on the first day's images and each day's images, and subsequently, final adjustment manually. MSHD and DSC were calculated using MIM Maestro between the first day and each day. Additionally, with reference to Fig. 3 in Ref. 10, the operator manually determined the center coordinates of the prostatic urethral ROI in axial images, and the displacement distance (Dd) was directly measured between the first day and each day image as follows:

$$Dd [\text{mm}] = \sqrt{(X_1 - X_n)^2 + (Y_1 - Y_n)^2}$$

where X and Y are the coordinates along the left–right and anterior–posterior directions, respectively. The center of the ROI on the first day was defined as coordinates X_1 and Y_1 , and the center of the ROI on other days was defined as coordinates X_n and Y_n . These metrics were calculated for the whole prostatic urethra and subgroups of the superior, middle, and inferior segments; each segment was defined as one-third of the evenly divided whole prostatic urethra following the previous study.¹⁰

Statistical analyses

We presented the results as mean \pm standard deviation, and used the Wilcoxon signed-rank test to compare the results for urethral identification in 2D- and 3D-T2W images. We used weighted kappa statistic to calculate interobserver agreement of visual assessment in addition to the following interpretation of kappa coefficients: <0.20 = slight, 0.21 – 0.40 = fair, 0.41 – 0.60 = moderate, 0.61 – 0.80 = good, and 0.81 – 1.00 = excellent.²⁶ Furthermore, Mann–Whitney U test was used to compare the results regarding interfractional motion between CT and MRI. $P < 0.05$ was considered statistically significant. We performed all statistical analyses using SPSS software (SPSS for Windows, version 28, IBM).

RESULTS

Urethral identification

To investigate the usefulness of 3D-MRI for urethral identification, we quantitatively and qualitatively compared the images from catheter CT, 2D- and 3D-MRI (without a catheter). Representative 2D- and 3D-T2W images are shown in Fig. 1. The prostatic urethra was identified as a high-intensity tract on T2W image without a catheter. Table 2 summarizes all values (mean \pm standard deviation) for interoperator variability of urethral identification in 2D- and 3D-T2W sequences and catheter CT. The 3D-T2W sequence showed significantly better urethral

identification than those of the 2D-T2W but was not comparable to catheter CT. Note that the patient groups for MRI and CT are different. In the visual assessment, the mean \pm standard deviation values for 2D- and 3D-T2W sequences were 2.2 ± 0.4 and 2.9 ± 0.3 , respectively ($P = 0.008$). Interobserver agreement was rated as good ($\kappa = 0.71$).

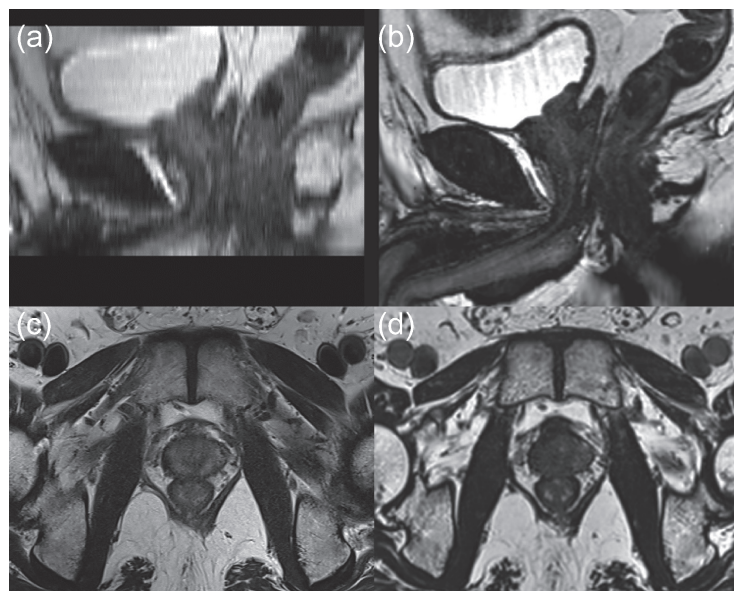


Fig. 1 Representative images of 2D- and 3D-MRI without a catheter

Fig. 1a: Reconstructed sagittal view of 2D-MRI

Fig. 1b: Reconstructed sagittal view of 3D-MRI

Fig. 1c: Transverse view of 2D-MRI

Fig. 1d: Reconstructed transverse view of 3D-MRI

The prostatic urethra was identified as a high-intensity tract on MRI. The 2D image acquired in the transverse, and sagittal views was reconstructed. The 3D image was acquired in the coronal, and the sagittal and transverse views were reconstructed.

2D: two-dimensional

3D: three-dimensional

MRI: magnetic resonance imaging

Table 2 Mean \pm standard deviation for urethral identification in MRI without a catheter and CT with a catheter

	MSHD [mm]		DSC	
2D MRI	0.58 ± 0.17		0.63 ± 0.10	
3D MRI	0.38 ± 0.09	$P = 0.002$	0.74 ± 0.05	$P = 0.002$
Catheter CT	0.12 ± 0.03		0.93 ± 0.02	

$P < 0.05$ was considered statistically significant. Note that the patient groups for MRI and CT are different.

MSHD: mean slice-wise Hausdorff distance

DSC: dice similarity coefficient

2D: two-dimensional

3D: three-dimensional

MRI: magnetic resonance imaging

CT: computed tomography

Interfractional motion

To provide the interfractional motion of the prostatic urethra, we obtained and analyzed the urethral position using CT with a catheter and 3D-MRI without a catheter over multiple days. Figure 2 contains box plots that compare CT and MRI for interfractional motion. MSHD values of MRI were smaller than those of CT, although there was no statistically significant difference. There was no statistically significant difference in DSC values between CT and MRI. The Dd values of MRI were significantly smaller than those of CT in the whole prostatic urethra, superior, and middle segments. Additionally, the value of MRI in the inferior segment was also smaller than that of CT, although there was no statistically significant difference. The superior segment in CT showed large variability and/or outliers compared with the other segments. Figure 3 shows the displacement map of the urethral center coordinates for the interfractional motion in CT with a catheter and MRI without a catheter. The maximum displacements of superior, middle, and inferior segments in CT were 6.6, 4.3, and 2.6 mm in the anterior–posterior direction and 3.1, 2.4, and 2.0 mm in the left–right direction, respectively. The maximum displacements of superior, middle, and inferior segments in MRI were 2.8, 2.2, and 2.0 mm in the anterior–posterior direction and 1.9, 1.7, and 2.0 mm in the left–right direction, respectively. Altogether, these data indicate that catheter CT had larger interfractional motion than catheter-free MRI and larger outliers and variability for all metrics, especially in the superior segment. Representative cases are shown in Fig. 4.

3D-MRI for urethra in prostate SBRT

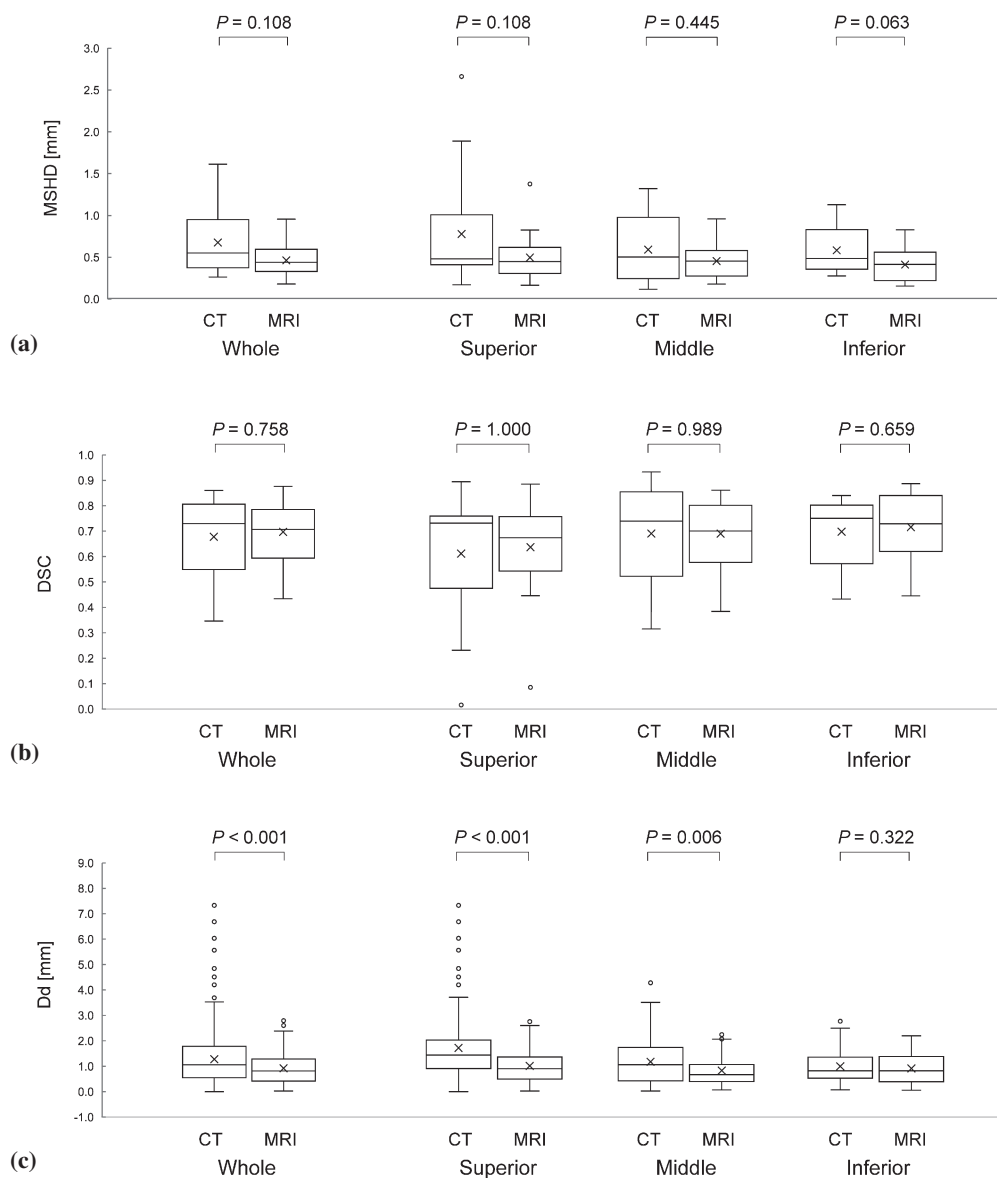


Fig. 2 Box plots showing the comparison of CT and MRI for interfractional motion

Fig. 2a: Mean slice-wise Hausdorff distance

Fig. 2b: Dice similarity coefficient

Fig. 2c: Displacement distance

$P < 0.05$ was considered significant. The cross indicates the mean value.

CT: computed tomography

MRI: magnetic resonance imaging

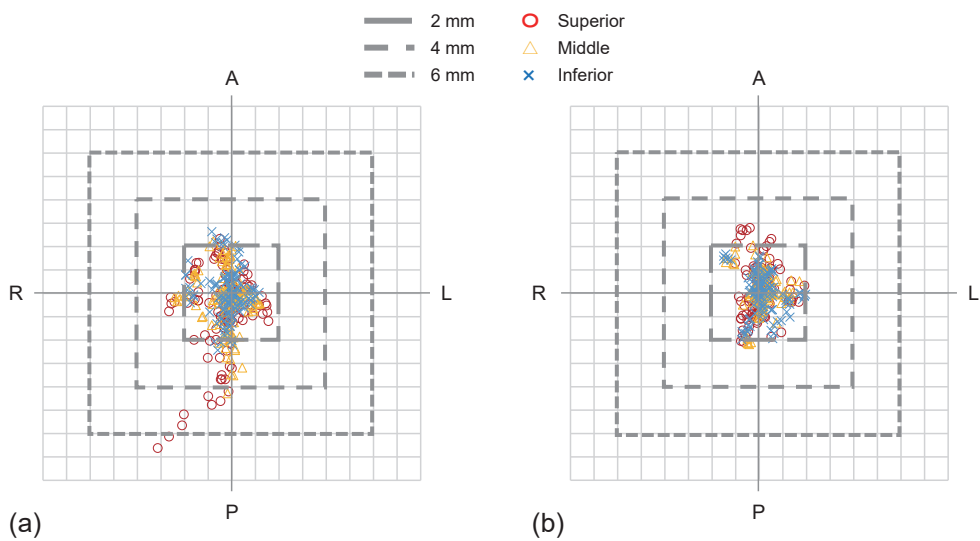


Fig. 3 Displacement map of the urethral center coordinates for the interfractional motion

Fig. 3a: CT with a catheter

Fig. 3b: MRI without a catheter

A: anterior

P: posterior

L: left

R: right

CT: computed tomography

MRI: magnetic resonance imaging

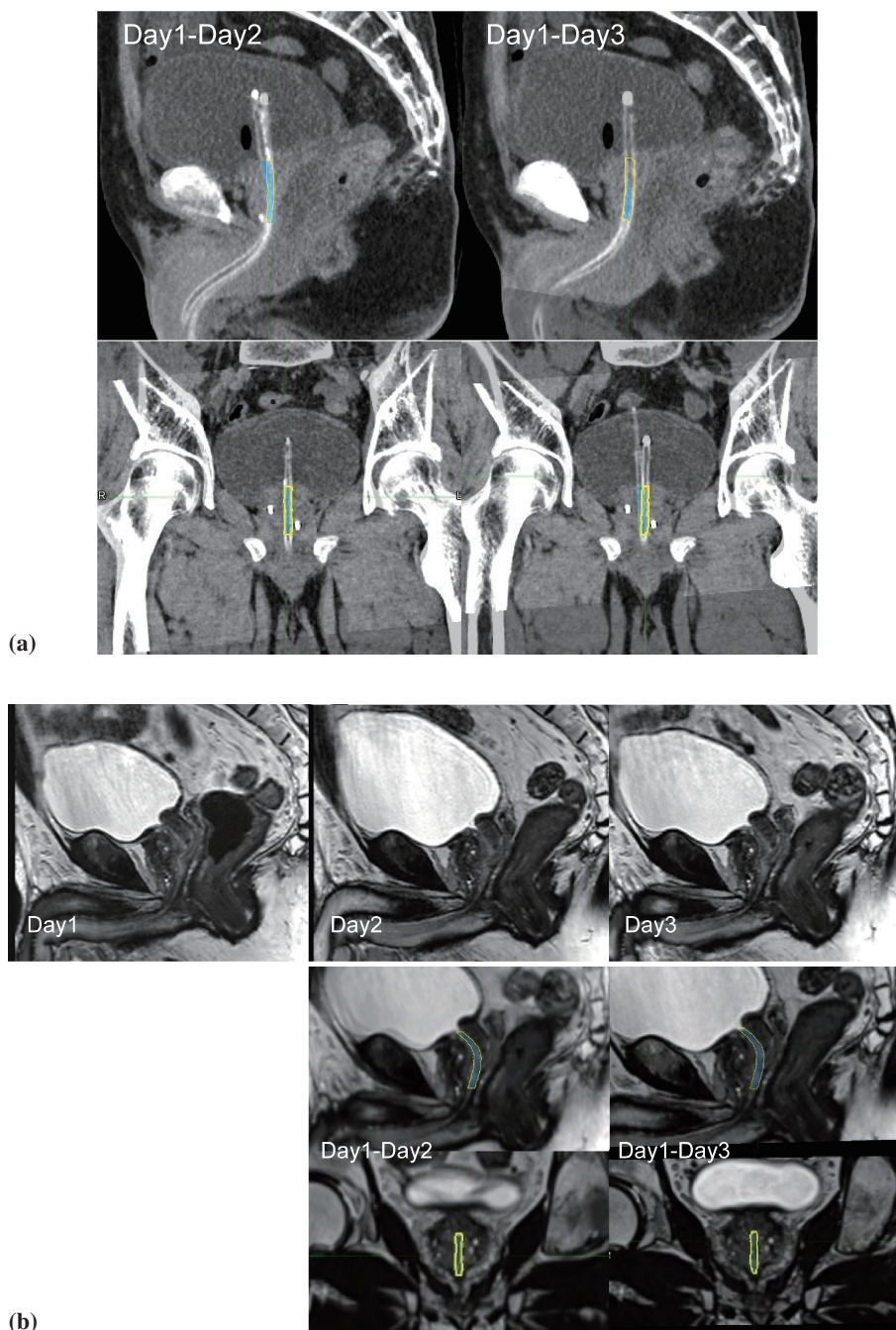


Fig. 4 Representative cases of CT with a catheter and MRI without a catheter
Fig. 4a: The yellow represents the urethral contouring on the first day CT, and the blue represents each day's contouring. The displacements are significant in the superior segment.

Fig. 4b: The yellow represents the urethral contouring on the first day MRI, and the blue represents each day's contouring. The urethral positions are relatively well matched.

CT: computed tomography

MRI: magnetic resonance imaging

DISCUSSION

Visualization of the prostatic urethra is important for urethral-sparing radiotherapy planning in prostate SBRT. We showed the usefulness of the 3D-T2W-SPACE sequence compared with 2D-T2W-TSE (in accordance with PI-RADS recommended parameters) for urethral identification without catheter insertion. Furthermore, we provided fundamental data for the interfractional motion using CT with a catheter and MRI without a catheter, suggesting that the interfractional motion in MRI was smaller than that of catheter CT.

In the urethral identification with catheter-free MRI, our results of MSHD and DSC using 3D-T2W images were comparable with the 2D-T2W results of the previous study.²⁰ The mean MSHD values were 0.44 and 0.39 mm in the previous 2D and our 3D sequences, respectively. In addition, mean DSC values were 0.75 and 0.74 in the previous 2D and our 3D sequences, respectively. Yoshimura et al's approach²⁰ has the originality of posturination imaging for generating a high contrast on T2W images due to the increase in signal intensity of the urethra, which resulted in adequate urethral identification. However, the disadvantages are that the bladder volume is different from CT, and urinating just before MRI may also change the shape of the surrounding organs, which will be a problem during CT-MRI registration. The 3D-T2W sequence can overcome these weaknesses with adequate identification performance. Moreover, the utilization of high bandwidth and nearly isovoxel ($\leq 1\text{mm}$) acquisitions in 3D sequence allow for less geometric distortion and multiplanar reconstruction, which may be helpful to geometrically identify accurate urethral position. Recently, MR-only treatment planning for radiation therapy has attracted huge attention.^{17,27,28} As the 3D-T2W image is widely used not only for urethral identification but also for prostate edge contouring,¹⁷ it would be a great advantage to use it for treatment planning and preirradiation check to provide anatomical information without physical and psychological burden to the patient. Although the CT scan time is very short, catheter insertion consumes the preparation and procedural time and manpower. By contrast, the 3D MR images used in our study can be obtained in about 7 min, and the acquisition times have been shortened increasingly because of technical developments²⁹; hence, the use of MRI would increase for radiotherapy.

However, the results of catheter CT had the highest score, which even the 3D sequence did not reach. In the visual assessment, although most of our cases with 3D-T2W images had scores of 3, which means adequate urethral identification is possible with no effect on contouring, it did not obtain a score of 4 in all cases because the observers already had the knowledge that the urethra could be clearly identified by catheter CT. Hence, the 3D-T2W sequence does not give optimum performance but the minimum level required has been achieved. A future challenge is needed to explore more sophisticated MR sequences for achieving optimum urethral identification comparable with catheter CT.

Regarding interfractional motion, the MSHD and Dd values in CT with a catheter were larger than those in MRI without a catheter, with a much larger variability and more outliers. These findings indicate that the prostatic urethral position may shift drastically from the original position due to differences in insertion procedure depending on the day because of catheter rigidity. Some previous studies have indicated that the urethral position with a catheter is often shifted to the anterior from the geometric center of the prostate.^{10,11} Dekura et al investigated the difference between the Foley catheter and guide-wire alone in the prostatic urethra and showed that the urethral position was often shifted to the anterior direction due to catheter insertion.¹⁰ Their results indicated that the maximum shift occurred in the superior segment 8.3 mm to the anterior direction. The displacement map (Fig. 3) shows a large variation in the superior segment, and the displacement is more remarkable in the anterior-posterior direction. These trends are consistent with those in a previous study.¹⁰ Some previous studies applying urethra-sparing techniques

have defined the prostatic urethra using a catheter plus a 3-mm isotropic margin and showed a low toxicity profile.^{30,31} Therefore, the variability and outliers in our results are major clinical problems because the outliers for the urethral position cannot be neglected on each irradiation day. In clinical practice, significant urethral displacements require replanning and rescheduling of radiotherapy. This is a critical concern, and it should be noted that SBRT with catheter CT may cause large displacements of the urethral position.

With MRI, as expected, the original urethral position obtained by catheter-free MRI resulted in small daily variations owing to the lack of external stress. To our knowledge, this is the first data to investigate the interfractional motion using 3D-MRI without a catheter. Since the MRI displacements in our results were within 3 mm, daily preirradiation image checks may be skipped by considering daily variations in margin settings in the future. One concern is that urethral identification is not perfect compared with catheter CT; therefore, uncertainty in identification may have affected the results of interfractional motion. However, there is no risk of problematic displacement in multiday irradiation (eg, replanning due to significant catheter displacement), which would be a great advantage. The bladder volume is another question. The bladder volume in CT can be kept exactly constant daily by infusing saline into the bladder using a catheter, which is one of the advantages. In MRI, it might be difficult to set the bladder volume completely constant, even if the images were obtained with the same waiting time after urination each day. However, a slightly different bladder volume each day would not be a serious problem because the main purpose of urine storage is to keep the bowel away from the prostate. Additionally, ultrasonography may help solve the problem by surveying the bladder volume.

Both approaches have advantages and disadvantages. Catheter CT allows 1) perfect urethral identification and 2) adjustment of the same bladder volume on each irradiation day. However, 1) there are large daily variations in the urethral position and 2) catheterization causes patient discomfort and is labor intensive. By contrast, MRI 1) is catheter-free radiotherapy that can save time and effort for catheterization and reduce unnecessary CT scans and 2) has small daily variations. However, MRI 1) has inferior urethral identification to catheter CT and 2) it is difficult to keep the same bladder volume on each irradiation day. We do not have a clear answer as to which is the superior approach, but we can have options by understanding the characteristics of both methods. Various studies are expected to provide sufficient evidence to determine which is the better approach.

There are some limitations to this study. First, because of the retrospective study, the patient groups evaluated for interfractional motion differed between CT and MRI, and the investigations were conducted over only 3 days. A prospective study is needed in the future to conduct a CT with a catheter and MRI without a catheter on the same subject over a longer period (ie, more than the actual SBRT period). Second, some subjective aspects could not be excluded from the analysis process for interfractional motion. The image registration of each day and the determination of urethral center coordinates were not fully automated. These subjective routines could have affected the results. Future study is desirable to automate the entire process of eliminating operator bias. Third, the investigation with MRI was conducted only under certain acquisition parameters. Since parameter optimization was out of scope in this study, we used typical parameters. Sequence optimization may improve the results of urethral identification and provide more precise data on interfractional motion, which is a future challenge.

CONCLUSION

Our findings in this study indicated that the 3D-T2W sequence had adequate prostatic urethral identification, and catheter-free MRI had less interfractional motion compared with catheter CT, which implies the feasibility as a noninvasive manner for prostate SBRT using MRI without a catheter. Further study is needed to develop more sophisticated MRI sequences for optimized visualization of the prostatic urethra.

AUTHOR CONTRIBUTIONS

YK and SO contributed equally to this work.

ACKNOWLEDGMENTS

This study was supported in part by Grant-in-Aid for scientific research from the Japanese Society for the Promotion of Science (JSPS KAKENHI, numbers 21H04296 to YK.)

DISCLOSURE STATEMENT

The authors declare that they have no conflicts of interest.

REFERENCES

- 1 Shimizu S, Nishioka K, Suzuki R, et al. Early results of urethral dose reduction and small safety margin in intensity-modulated radiation therapy (IMRT) for localized prostate cancer using a real-time tumor-tracking radiotherapy (RTRT) system. *Radiat Oncol.* 2014;9:118. doi:10.1186/1748-717X-9-118.
- 2 Repka MC, Guleria S, Cyr RA, et al. Acute urinary morbidity following stereotactic body radiation therapy for prostate cancer with prophylactic alpha-adrenergic antagonist and urethral dose reduction. *Front Oncol.* 2016;6:122. doi:10.3389/fonc.2016.00122.
- 3 Tanaka O, Hayashi S, Matsuo M, et al. Comparison of MRI-based and CT/MRI fusion-based postimplant dosimetric analysis of prostate brachytherapy. *Int J Radiat Oncol Biol Phys.* 2006;66(2):597–602. doi:10.1016/j.ijrobp.2006.06.023.
- 4 Bowes D, Crook JM, Rajapakshe R, Araujo C, Parker B. Defining a magnetic resonance scan sequence for permanent seed prostate brachytherapy postimplant assessment. *Brachytherapy.* 2013;12(1):25–29. doi:10.1016/j.brachy.2012.03.001.
- 5 Amdur RJ, Gladstone D, Leopold KA, Harris RD. Prostate seed implant quality assessment using MR and CT image fusion. *Int J Radiat Oncol Biol Phys.* 1999;43(1):67–72. doi:10.1016/S0360-3016(98)00372-1.
- 6 Hoskin PJ, Colombo A, Henry A, et al. GEC/ESTRO recommendations on high dose rate afterloading brachytherapy for localised prostate cancer: an update. *Radiother Oncol.* 2013;107(3):325–332. doi:10.1016/j.radonc.2013.05.002.
- 7 Hooton TM, Bradley SF, Cardenas DD, et al. Diagnosis, prevention, and treatment of catheter-associated urinary tract infection in adults: 2009 international clinical practice guidelines from the Infectious Diseases Society of America. *Clin Infect Dis.* 2010;50(5):625–663. doi:10.1086/650482.
- 8 Saint S. Clinical and economic consequences of nosocomial catheter-related bacteriuria. *Am J Infect Control.* 2000;28(1):68–75. doi:10.1016/S0196-6553(00)90015-4.
- 9 Leuck AM, Wright D, Ellingson L, Kraemer L, Kuskowski MA, Johnson JR. Complications of Foley catheters — is infection the greatest risk? *J Urol.* 2012;187(5):1662–1666. doi:10.1016/j.juro.2011.12.113.
- 10 Dekura Y, Nishioka K, Hashimoto T, et al. The urethral position may shift due to urethral catheter place-

- ment in the treatment planning for prostate radiation therapy. *Radiat Oncol.* 2019;14(1):226. doi:10.1186/s13014-019-1424-8.
- 11 Anderson C, Lowe G, Ostler P, et al. I-125 seed planning: an alternative method of urethra definition. *Radiother Oncol.* 2010;94(1):24–29. doi:10.1016/j.radonc.2009.11.003.
 - 12 Litzenberg DW, Muenz DG, Archer PG, et al. Changes in prostate orientation due to removal of a Foley catheter. *Med Phys.* 2018;45(4):1369–1378. doi:10.1002/mp.12830.
 - 13 Waterman FM, Dicker AP. Determination of the urethral dose in prostate brachytherapy when the urethra cannot be visualized in the postimplant CT scan. *Med Phys.* 2000;27(3):448–451. doi:10.1118/1.598912.
 - 14 Lee HK, D'Souza WD, Yamal JMJ, et al. Dosimetric consequences of using a surrogate urethra to estimate urethral dose after brachytherapy for prostate cancer. *Int J Radiat Oncol Biol Phys.* 2003;57(2):355–361. doi:10.1016/S0360-3016(03)00583-2.
 - 15 Kataria T, Gupta D, Goyal S, et al. Simple diagrammatic method to delineate male urethra in prostate cancer radiotherapy: an MRI based approach. *Br J Radiol.* 2016;89(1068):20160348. doi:10.1259/bjr.20160348.
 - 16 Schmidt MA, Payne GS. Radiotherapy planning using MRI. *Phys Med Biol.* 2015;60(22):R323–R361. doi:10.1088/0031-9155/60/22/R323.
 - 17 Kapanen M, Collan J, Beule A, Seppälä T, Saarilahti K, Tenhunen M. Commissioning of MRI-only based treatment planning procedure for external beam radiotherapy of prostate. *Magn Reson Med.* 2013;70(1):127–135. doi:10.1002/mrm.24459.
 - 18 Zakian KL, Wibmer A, Vargas HA, et al. Comparison of motion-insensitive T2-weighted MRI pulse sequences for visualization of the prostatic urethra during MR simulation. *Pract Radiat Oncol.* 2019;9(6):e534–e540. doi:10.1016/j.prro.2019.06.009.
 - 19 Rai R, Sidhom M, Lim K, Ohanessian L, Liney GP. MRI micturating urethrography for improved urethral delineation in prostate radiotherapy planning: a case study. *Phys Med Biol.* 2017;62(8):3003–3010. doi:10.1088/1361-6560/62/8/3003.
 - 20 Yoshimura T, Nishioka K, Hashimoto T, et al. Visualizing the urethra by magnetic resonance imaging without usage of a catheter for radiotherapy of prostate cancer. *Phys Imaging Radiat Oncol.* 2021;18:1–4. doi:10.1016/j.phro.2021.03.002.
 - 21 Weinreb JC, Barentsz JO, Choyke PL, et al. PI-RADS prostate imaging-reporting and data system: 2015, version 2. *Eur Urol.* 2016;69(1):16–40. doi:10.1016/j.eururo.2015.08.052.
 - 22 Gupta RT, Spilseth B, Patel N, Brown AF, Yu J. Multiparametric prostate MRI: focus on T2-weighted imaging and role in staging of prostate cancer. *Abdom Radiol(NY).* 2016;41(5):831–843. doi:10.1007/s00261-015-0579-5.
 - 23 Polanec SH, Lazar M, Wengert GJ, et al. 3D T2-weighted imaging to shorten multiparametric prostate MRI protocols. *Eur Radiol.* 2018;28(4):1634–1641. doi:10.1007/s00330-017-5120-5.
 - 24 Rosenkrantz AB, Neil J, Kong X, et al. Prostate cancer: comparison of 3D T2-weighted with conventional 2D T2-weighted imaging for image quality and tumor detection. *AJR Am J Roentgenol.* 2010;194(2):446–452. doi:10.2214/AJR.09.3217.
 - 25 Mugler JP 3rd. Optimized three-dimensional fast-spin-echo MRI. *J Magn Reson Imaging.* 2014;39(4):745–767. doi:10.1002/jmri.24542.
 - 26 Landis JR, Koch GG. The measurement of observer agreement for categorical data. *Biometrics.* 1977;33(1):159–174. doi:10.2307/2529310.
 - 27 Jonsson J, Nyholm T, Söderkvist K. The rationale for MR-only treatment planning for external radiotherapy. *Clin Transl Radiat Oncol.* 2019;18:60–65. doi:10.1016/j.ctro.2019.03.005.
 - 28 Bird D, Henry AM, Sebag-Montefiore D, Buckley DL, Al-Qaisieh B, Speight R. A systematic review of the clinical implementation of pelvic magnetic resonance imaging-only planning for external beam radiation therapy. *Int J Radiat Oncol Biol Phys.* 2019;105(3):479–492. doi:10.1016/j.ijrobp.2019.06.2530.
 - 29 Wong OL, Poon DMC, Kam MKM, et al. 3D-T2W-TSE radiotherapy treatment planning MRI using compressed sensing acceleration for prostate cancer: image quality and delineation value. *Asia Pac J Clin Oncol.* 2022;18(5):e369–e377. doi:10.1111/ajco.13752.
 - 30 Zilli T, Jorcano S, Bral S, et al. Once-a-week or every-other-day urethra-sparing prostate cancer stereotactic body radiotherapy, a randomized phase II trial: 18 months follow-up results. *Cancer Med.* 2020;9(9):3097–3106. doi:10.1002/cam4.2966.
 - 31 Jaccard M, Zilli T, Dubouloz A, et al. Urethra-sparing stereotactic body radiation therapy for prostate cancer: quality assurance of a randomized phase 2 trial. *Int J Radiat Oncol Biol Phys.* 2020;108(4):1047–1054. doi:10.1016/j.ijrobp.2020.06.002.